Assessment of Base Capacity of Open-ended Tubular Piles Installed by the Rotary Cutting Press-in Method

Yukihiro ISHIHARA[i], Stuart HAIGH[ii] and Junichi KOSEKI[iii]

[i] Manager, Scientific Research Section, GIKEN LTD., Japan. (ishihara@giken.com)
[ii] Senior Lecturer, Department of Engineering, University of Cambridge, UK. (skh20@cam.ac.uk)
[iii] Professor, Department of Civil Engineering, The University of Tokyo, Japan. (koseki@civil.t.u-tokyo.ac.jp)

Abstract

The 'press-in' method is a piling technique that installs piles with a static jacking force while obtaining a reaction force from previously installed piles. The applicable ground conditions of this method have been significantly expanded by the 'Rotary Cutting Press-in (RCP)' method, whereby a vertical jacking force and a torque are applied simultaneously onto a pile with cutting teeth on its base while water is injected around the pile base. In this paper, a method to estimate the base capacity of RCP piles is proposed based on UWA-05 framework. The proposed method utilizes CPT or SPT results as input parameters and estimates the plugging condition (Incremental Filling Ratio, *IFR*) from these results. Four static load tests on open-ended RCP piles were shown to be well-predicted by the proposed method in terms of the base capacity, regardless of the embedment depth into a bearing stratum.

Key words: Rotary Cutting Press-in, Base capacity, Open-ended pile (IGC: E04/K07)

1. Introduction

In the Press-in Method (International Press-in Association (IPA), 2016), a static jacking force is used to install a pile while a reaction force is obtained from previously installed piles. The environmental impacts of noise and vibration are thus lower than those for conventional piling methods, and the space for piling and cost of temporary works can be significantly reduced. Recently, a technique called 'Rotary Cutting Press-in' (RCP) has been developed, expanding the applicability of the Press-in Method to hard ground. In RCP, vertical and rotational jacking forces are applied simultaneously to a pile with teeth on its base. Low-pressure water injection (as opposed to water jetting) is usually conducted during the penetration process to reduce the penetration resistance and facilitate the piling work. A typical water injection system is described in IPA (2016).

Since the Press-in Method is a relatively new piling method, and is more frequently used for construction of walls in which the horizontal performance is most important, there has until recently been a lack of design methods for the axial capacity of piles installed using this method. Deeks & White (2007) argued that the axial stiffness of jacked piles (including those installed by Standard Press-in without water jetting or augering) measured in their centrifuge tests as well as in the field load tests of Dingle (2006) was higher than that of driven or bored piles estimated by existing methods. White & Deeks (2007) proposed a CPT-based method to estimate the axial capacity of jacked piles by modifying the values of coefficients in the UWA-05 framework for driven piles (Xu *et al*., 2008). This suggested that jacked piles exhibit a higher capacity than driven piles, if the capacity is defined as the resistance when the pile base displacement reaches one-tenth of the outer diameter of the pile. The higher stiffness and capacity of jacked piles are attributed to the loading history; the static loading and unloading at the end of installation leading to a stiffer response at the pile base when the pile is subsequently load tested (White *et al*., 2010).

Hirata *et al*. (2009) collected field load test results of three RCP piles, most of which had a relatively small embedment depth into a bearing stratum, and discussed the applicability of an SPT-based design method (Japan Road Association (JRA), 2002). They confirmed that the measured capacity was greater than the estimated values for driven piles, while the measured stiffness fell between the estimated values for driven and bored piles. White *et al*. (2010) analyzed one of the three field load test results of Hirata *et al*. (2009) and confirmed that the measured base capacity fell in between the estimated values for driven and bored piles using UWA-05. These analyses, together with the fact that the embedment depth of the load tested piles into a bearing stratum was relatively small, suggest that the effect of loading history, which is a source of the high base response of jacked piles, can also be expected for RCP piles.

IPA (2014) summarized the results of Hirata *et al*. (2009) and presented methods to estimate the capacity and stiffness of RCP piles, by referring to those for driven and bored piles specified by JRA (2012). According to the comparison of the measured and the estimated base capacity provided in IPA (2014), the method provides very conservative values for the base capacity. JRA (2012) was revised in 2017 (JRA, 2017), and the applicability of JRA (2017) to RCP piles is unknown.

This paper focuses on the base capacity of an RCP pile, and (1) gives an overview on the existing method to estimate the base capacity of an RCP pile, (2) proposes a new estimation method and (3) assesses the validity of the proposed method by comparing with field test results.

2. Existing method to estimate the base capacity of RCP piles

The base capacity of an open-ended pile ($Q_{b,0.1Do}$), generally defined as the base resistance when the pile base has been displaced a distance equivalent to one-tenth of its outer diameter (D_o), is usually estimated by multiplication of a unit base capacity at the corresponding base displacement ($q_{b,0.1Do}$) and the gross (closed-ended) cross-sectional area ($A_{b,closed}$). In other words, $q_{b,0.1Do}$ is taken as an apparent unit base capacity reflecting the plugging condition of an open-ended pile, being the average of the stress of the soil on the pile annulus ($q_{bp,0.1Do}$) and the resistance of the soil beneath the soil column inside the pile ($q_{bi,0.1Do}$). These symbols are illustrated in Fig. 1, together with those for the inner diameter of a pile (D_i), the depth of the pile base (z), the embedment depth into the bearing stratum (z_{bs}) and the length of the soil column inside the pile (h).

It is often the case that piles are embedded into a bearing stratum with a sufficient strength and thickness to secure their vertical bearing performance. As the pile 'feels' the strength of soils not only beneath but also above its base, some embedment depth into the bearing stratum (z_{bs}) is necessary to mobilize the full strength of that layer (Meyerhoff & Valsangkar, 1977; White & Bolton, 2005). In addition, the plug strength (= $q_{bi,0.1Do}$) also varies with z_{bs}. These issues of the partial embedment into the bearing stratum and the plugging condition have been considered in existing design codes in different ways.

According to IPA (2014), the base capacity of an RCP pile can be safely estimated by equations (1) and (2):

$$Q_{b,0.1Do} = A_{b,closed} \times q_{b,0.1Do} \tag{1}$$

$$q_{b,0.1Do} = 60 \times \min(N_{a1}, 40) \tag{2}$$

where N_{a1} is the so-called 'bearing stratum N value' obtained by using SPT N values recorded in the depth range from the pile base to $4D_o$ above the pile base (JRA, 2012). These expressions were obtained by modifying methods for driven piles recommended by JRA (2012), taking into account that z_{bs} is recommended to be equivalent to D_o (IPA, 2014), determined from the viewpoint of securing the capacity while assuring piling efficiency.

In JRA (2012), the base capacity of open-ended tubular driven piles can be estimated by equations (1) and (3):

$$q_{b,0.1Do} = 300 \times \min\left(\frac{z_{bs}}{5D_o}, 1\right) \times \min(N_{a1}, 40) \tag{3}$$

Equation (3) implies that the unit base capacity ($q_{b,0.1Do}$) is reduced from the fully mobilized case ($z_{bs} = 5D_o$) linearly with z_{bs} , as shown in Fig. 2, incorporating the effect of partial embedment into the bearing stratum and the plugging condition. Equation (3) is similar to equation (2) if z_{bs} is taken as equivalent to D_o, as required by IPA (2014).

JRA (2012) was revised in 2017, and the concept of reducing the unit base capacity with the value of z_{bs} was removed (JRA, 2017). Instead, z_{bs} is required to be greater than or equal to $2D_o$, and if this requirement is satisfied, $q_{b,0.1Do}$ is consistently expressed as:

$$q_{b,0.1Do} = \begin{cases} 90 \times \min(N_{a2}, 50) & \text{(Cohesive soil)} \\ 130 \times \min(N_{a2}, 50) & \text{(Sand, Sand and gravel)} \end{cases} \tag{4}$$

where N_{a2} is the bearing stratum N value obtained by averaging the SPT N values in the depth range from the pile base to $3D_o$ below the pile base. As RCP piles are usually embedded by D_o, JRA (2017) cannot be applied to RCP piles.

3. A new method to estimate the base capacity of RCP piles

3.1. Framework of the proposed method

The Rotary Cutting Press-in method is usually adopted when the ground is hard, containing gravels or cobbles or consisting of rocks. The framework of the proposed method will be based on UWA-05 (CPT-based), but due to the lower applicability of CPT to such hard ground conditions, SPT results will also be utilized as input parameters. A feature of the proposed method is the estimation of the plugging condition from the CPT or SPT results, without assuming values of z_{bs}.

According to White & Deeks (2007), the base capacity of jacked piles can be estimated by equations (1) and (5), based on the UWA-05 framework:

$$q_{b,0.1Do} = \left[0.15 + 0.75 \times \left\{1\text{-}FFR \times \left(\frac{D_i}{D_o}\right)^2\right\}\right] \times q_{c,ave} \tag{5}$$

where $q_{c,ave}$ is the cone resistance averaged by the Dutch method (Lehane *et al*., 2005) and *FFR* (Final Filling Ratio) is the value of *IFR* (Incremental Filling Ratio, expressed by equation (6)) at the end of pile installation.

$$IFR = \frac{dh}{dz} \tag{6}$$

Here, *dh* and *dz* are the increments of *h* and *z* over the length of installation being considered. In UWA-05, equation (7) is recommended to obtain *FFR*, if *h* is not measured.

$$FFR = \min\left(1,\ \left(\frac{D_i\ [\mathrm{m}]}{1.5\ [\mathrm{m}]}\right)^{0.2}\right) \tag{7}$$

According to White & Bolton (2005), the unit base capacity $q_{b,pl}$, defined by a plunging load (the load at which continued penetration occurs without any further increase in resistance), can be expressed as:

$$q_{b,pl} = 0.9 \times q_{c,ave} \tag{8}$$

regardless of D_o. On the other hand, in SPT-based methods, $q_{b,0.1Do}$ of closed-ended driven piles has been widely accepted in practice as:

$$q_{b,0.1Do} = 300 \times \min(N, 50)\ [\mathrm{kPa}] \tag{9}$$

where the value of 300 is based on the findings of Meyerhoff (1956) and the load test data of Kerisel (1961) and the BCP Committee (1971) (AIJ, 2001). Assuming $q_{b,pl} = q_{b,0.1Do}$, equations (8) & (9) give:

$$q_{c,ave} \approx 333 \times \min(N, 50)\ [\mathrm{kPa}] \tag{10}$$

and equation (5) can be written as:

$$q_{b,0.1Do} \approx 333 \times \left[0.15 + 0.75 \times \left\{1\text{-}FFR \times \left(\frac{D_i}{D_o}\right)^2\right\}\right] \times \min(N, 50)\ \ [\mathrm{kPa}] \tag{11}$$

As $q_{b,pl}$ will be greater than $q_{b,0.1Do}$, equation (11) would provide a more conservative estimation of results than equation (5).

3.2. Estimation of IFR and FFR in axial jacking

The plugging condition of a tubular pile is governed by the equilibrium of the soil within it. Following the analysis method of Randolph *et al*. (1991), this equilibrium can be investigated based on a series of infinitesimally thin disks. The disk of soil at the bottom of the soil column inside the pile, with a thickness of *dh*, will be considered here, as shown in Fig. 3. During static penetration, this disk experiences a base stress (q_{bi}) from the soil beneath, resisted by a frictional stress (τ_i) mobilized at the soil-pile interface inside the pile, the weight of the disk and the stress on its top surface. The frictional stress mobilized can be related to the base stress by:

$$\tau_i = \beta \times q_{bi}' \tag{12}$$

where q_{bi}' is an effective base stress (obtained by subtracting pore water pressure from q_{bi}) and β is the coefficient linking q_{bi}' and τ_i. On the upper surface of disk in Fig. 3, a vertical stress (p) will act which is derived from the weight of the soil above and the integrated stresses arising from the soil-pile friction. This stress could be assumed to be equal to the maximum previously observed base stress (q_{BI}).

The equilibrium of forces acting on the disk can hence be expressed as:

$$\frac{\pi \times D_i^2}{4} \times q_{bi} = (\pi \times D_i \times dh) \times (\beta \times q_{bi}') + \frac{\pi \times D_i^2}{4} \times (\gamma \times dh) + \frac{\pi \times D_i^2}{4} \times q_{BI} \tag{13}$$

where γ is the unit weight of soil. Assuming the pore water pressure at the pile base to be $\gamma_w \times h$ (where γ_w is the unit weight of water), it can be shown that:

$$q_{bi} = \frac{q_{BI} + \gamma \times dh - \frac{4\beta}{D_i} \times dh \times \gamma_w \times h}{1 - \frac{4\beta}{D_i} \times dh} \tag{14}$$

Randolph *et al*. (1991) solved this equation directly by assuming that maximum friction is always mobilized within the soil plug, however this has been found to overestimate the observed base stress unless an adequate ‘effective length’ through which the friction is mobilized is found. As the ratio of the base stress (q_{bi}) to CPT cone resistance (q_c) has been shown by Lehane & Gavin (2001) to vary in proportion to *IFR* (equation 14), this can be used along with equilibrium of the soil element to achieve an alternative analysis.

$$q_{bi} = \lambda \times q_c \times (1 - IFR) \tag{15}$$

where λ is a coefficient assumed as 0.9 based on Fig. 4. Combining equations (14) and (15), *IFR* is expressed as:

$$IFR = 1 - \frac{q_{\mathrm{BI}} + \gamma \times dh - \frac{4\beta}{D_{\mathrm{i}}} \times dh \times \gamma_{\mathrm{w}} \times h}{\left(1 - \frac{4\beta}{D_{\mathrm{i}}} \times dh\right) \times \lambda \times q_{\mathrm{c}}} = \frac{dh}{dz} \tag{16}$$

With equations (9), (10) and the assumption of $q_{\mathrm{c}} = q_{\mathrm{c,ave}}$, equations (15) & (16) can be transformed for the SPT into:

$$\begin{cases} q_{\mathrm{bi}} = (1 - IFR) \times 300 \times \min(N, 50) & (17) \\ IFR = 1 - \dfrac{q_{\mathrm{BI}} + \gamma \times dh - \frac{4\beta}{D_{\mathrm{i}}} \times dh \times \gamma_{\mathrm{w}} \times h}{\left(1 - \frac{4\beta}{D_{\mathrm{i}}} \times dh\right) \times 300 \times \min(N, 50)} = \dfrac{d\square}{dz} & (18) \end{cases}$$

For any pile displacement increment *dz*, the increase in plug length *dh* can be calculated by solving equation (16) (CPT-based) or equation (18) (SPT-based). The installation process can thus be completely analysed by incremental calculations from a starting point of h=0 and q_{BI} =0 at z=0. This procedure is summarized in Fig. 5.

3.3. Estimation of IFR and FFR in Rotary Cutting Press-in

In Rotary Cutting Press-in, the friction at the soil-pile interface will act in both vertical and horizontal directions if the soil column does not rotate with the pile. The vertical friction inside the pile will be reduced as a result, which will mitigate the extent of plugging (White *et al*., 2010). According to Bond (2011), the friction vector on the outer pile surface acts in the direction of the relative motion between the pile and the soil. Applying this to friction inside the pile, and assuming that the inner soil column does not rotate, the vertical frictional stress in equation (12) will be:

$$\tau_{\mathrm{i}} = \beta \times \frac{1}{\sqrt{1 + (v_{\mathrm{r}}/v_{\mathrm{d}})^2}} \times q_{\mathrm{bi}}' \tag{19}$$

where v_{r} and v_{d} are rotational and vertical downward velocity of the pile. Equations (18) can be written as:

$$IFR = 1 - \frac{q_{\mathrm{BI}} + \gamma \times dh - \frac{4\beta}{D_{\mathrm{i}} \times \sqrt{1 + (v_{\mathrm{r}}/v_{\mathrm{d}})^2}} \times dh \times \gamma_{\mathrm{w}} \times h}{\left(1 - \frac{4\beta}{D_{\mathrm{i}} \times \sqrt{1 + (v_{\mathrm{r}}/v_{\mathrm{d}})^2}} \times dh\right) \times \lambda \times q_{\mathrm{c}}} \tag{20}$$

$$IFR = 1 - \frac{q_{\mathrm{BI}} + \gamma \times dh - \frac{4\beta}{D_{\mathrm{i}} \times \sqrt{1 + (v_{\mathrm{r}}/v_{\mathrm{d}})^2}} \times dh \times \gamma_{\mathrm{w}} \times h}{\left(1 - \frac{4\beta}{D_{\mathrm{i}} \times \sqrt{1 + (v_{\mathrm{r}}/v_{\mathrm{d}})^2}} \times dh\right) \times 300 \times \min(N, 50)} \tag{21}$$

The vertical stress from the above soil mobilized during RCP in equations (20) or (21) is smaller than that mobilized during axial jacking as a consequence of the reduction in the vertical frictional stress based on equation (19). During the subsequent load test (i.e. when the pile is vertically pushed without rotation after the end of RCP) the internal stresses will be greater than those during installation, due to the lack of rotation. Taking this into account, *IFR* during a load test carried out after the termination of RCP installation (i.e. *FFR* to be substituted into equation (5) or (11)) can be expressed as:

$$FFR = 1 - \frac{\left\{\left(q_{\mathrm{BI}} - \gamma \times h\right) \times \sqrt{1 + (v_{\mathrm{r}}/v_{\mathrm{d}})^2} + \gamma \times h\right\} + \gamma \times dh - \dfrac{4\beta}{D_{\mathrm{i}}} \times dh \times \gamma_{\mathrm{w}} \times h}{\left(1 - \dfrac{4\beta}{D_{\mathrm{i}}} \times dh\right) \times \lambda \times q_{\mathrm{c}}} \tag{22}$$

$$FFR = 1 - \frac{\left\{\left(q_{\mathrm{BI}} - \gamma \times h\right) \times \sqrt{1 + (v_{\mathrm{r}}/v_{\mathrm{d}})^2} + \gamma \times h\right\} + \gamma \times dh - \dfrac{4\beta}{D_{\mathrm{i}}} \times dh \times \gamma_{\mathrm{w}} \times h}{\left(1 - \dfrac{4\beta}{D_{\mathrm{i}}} \times dh\right) \times 300 \times \min(N, 50)} \tag{23}$$

The procedure for estimating *FFR* for RCP piles is summarized in Fig. 6.

4. Validation of the proposed estimation method based on experimental results

4.1. IFR during axial jacking of a model pile in dry sand

Kurashina (2016) carried out a model test on an axially jacked pile in which the model ground was prepared using air-pluviation of air-dry silica sand #6, to a relative density (D_{r}) of 60%, in a soil tank 1000mm square with a height of 1700mm. The depth of the model ground was 1650mm. The CPT profile of the model ground is shown in Fig. 7. An open-ended steel tubular pile with D_{o} = 101.6mm and D_{i} = 83.5mm was used as a test pile as shown in Fig. 8. This consisted of two concentric pipes with a load cell sandwiched between the heads of two pipes to measure the total frictional force on the inner pipe (Q_{si}). A stroke sensor (DP-1000E) was placed near the top of the inner pipe to measure the length of the inner soil column *h* using a wire attached to a steel weight on the surface of the inner soil. 320 grit sand paper was pasted on the inner surface of the inner pipe. The internal friction angle of the soil was confirmed to be 38.7 degrees at D_{r} = 60% by triaxial compression tests, and the friction angle at the soil-pile interface (δ_{sp}) was estimated as 33 degrees by a simple investigation shown in Fig. 9.

The calculation was carried out with *dz* = 0.01m using the CPT-based equations. Two methods were adopted to obtain β, one of which was based on equations (24) and (25) proposed by Randolph *et al*. (1991):

$$\beta = \frac{\sin\phi \times \sin\left(\Delta\text{-}\delta_{\mathrm{sp}}\right)}{1+\sin\phi \times \cos\left(\Delta\text{-}\delta_{\mathrm{sp}}\right)} \tag{24}$$

$$\Delta = \sin^{-1}\left(\frac{\sin\delta_{\mathrm{sp}}}{\sin\phi}\right) \tag{25}$$

These equations provide minimum values of β based on an assumption that the soil near the edge of the soil column is at active failure. An alternative is simply to introduce the coefficient of earth pressure (K) to express β as:

$$\beta = K \times \tan\delta_{sp} \quad (26)$$

Comparison of measured and estimated values of h and IFR are shown in Fig. 10. In the estimation, several K values (0.2, 0.4, 0.6, 0.8, 1.0 and 1.2) were adopted to investigate their influence on the results. It can be seen that adopting equations (24) leads to underestimation of h and overestimation of IFR by a factor of 3, while equation (26) provides reasonable results when K is taken as 1.0.

Fig. 11 shows a comparison of measured and estimated q_{bi}, where measured q_{bi} is obtained by dividing the measured Q_{si} by ($\pi D_i^2/4$). Together with Fig. 10, it can be confirmed that q_{bi} is underestimated if IFR is overestimated and vice versa, and that q_{bi} and IFR are estimated well if K is taken as 1.0 in equation (26). These corresponding trends in h, IFR and q_{bi} suggest the validity of the discussion in Section 3.2.

Fig. 12 shows a comparison of measured Q_{si}, measured Q (head load) and estimated $Q_{b,0.1Do}$. Ideally, $Q_{b,0.1Do}$ is expected to be between Q_{si} and Q. However, it is seen in Fig. 12 that equation (26) with K = 1.0, which provides the best matches in h, IFR and q_{bi}, leads to an overestimation of $Q_{b,0.1Do}$. One reason might be that in practical situations, IFR values during installation will be larger than those during the load test, partly because the higher penetration rate during installation causes higher excess pore water pressure and reduces friction at the soil-pile interface. As equation (5) implicitly accounts for this, applying IFR values measured (or accurately estimated) in dry sand to equation (5) will lead to the overestimation of $Q_{b,0.1Do}$.

4.2. Static load test results on full-scale RCP piles

Results of four static load tests on RCP piles were collected. Site profiles are shown in Fig. 13, where the profile in A-2016 was estimated from 12 SPT results around the test point. Pile specifications and installation conditions are shown in Table 1. During Rotary Cutting Press-in, a pile was installed with repeated penetration and extraction, where downward displacement (l_d) and upward displacement (l_u) was applied alternately. In addition, the upper limits of vertical jacking force (F_{UL}) and torque (T_{UL}) were manually set, and the pile was extracted by l_u if jacking force (F) or torque (T) reached their upper limits. Symbols n_T and f_w in Table 1 represent the number of teeth on the pile base and the flowrate of water injected near the pile base respectively. The values of v_d, v_u and v_r are nominal and can become smaller when the values of F or T increase. The load test conditions and the measured base capacity are summarized in Table 2, where t_{LT} is the elapsed time from the end of installation to the start of load test. Details of T-2007 and F-2008 can be found in Hirata *et al*. (2009) and IPA (2014), while those of A-2016 are reported by Ishihara *et al*. (2016).

In T-2007, F-2008 and N-2017, a pile with teeth on its base was installed by Rotary Cutting Press-in with water injection down to 0.9D_o or 1D_o above the final depth. The injection of water was then stopped (allowing minimal use if necessary) and Rotary Cutting Press-in was continued down to the final depth. At the end of installation, axial loading was conducted for a period of time. The jacking force and displacement recorded during this axial loading (F_t, l_t) are summarized in Table 1. In A-2016, a pile with teeth on its base was installed by Rotary Cutting Press-in without water injection to 2m below the ground, and was then pressed-in (axially jacked without rotation) to the final depth. In all tests, h was measured manually during installation intermittently or at the beginning and the end of installation, using a tape measure.

The load test conditions including the loading conditions were determined to follow the recommendations of JGS (2002), except for the shorter t_{LT} in A-2016 and the existence of adjacent piles within the distance of $3D_o$ from the center of the test pile in T-2007 and F-2008. The shorter t_{LT} will lead to lower pile capacity, but would not have significant influence on base capacity as the time effect is generally only significant for the pile shaft (e.g. Skov & Denver, 1988; Chow *et al*., 1998; White & Deeks, 2007). The existence of adjacent piles may lead to greater base capacity, considering the findings of Yetginer *et al*. (2006) where the penetration resistance increased with the increasing number of piles and that the group effect in terms of capacity was slightly greater than 1.

In the load test, base capacity ($Q_{b,0.1Do}$) was defined to be the axial load measured by the strain gauges attached to the inner surface near the pile base when the base displacement during the load test was $0.1D_o$. The position of the strain gauges was $1D_o$ above the pile base in T-2007, F-2008 and N-2017, and was $0.5D_o$ above the base in A-2016, which leads to greater measured values of $Q_{b,0.1Do}$ than when they are positioned at the base. On the other hand, in all the tests, strain gauge readings were offset to be zero just before the start of the load test. This leads to the uncertainty of the residual load at the pile base after the pile was installed down to the final depth. As a result, the measured values of $Q_{b,0.1Do}$ are likely to be smaller than the actual values, as suggested by many researchers (e.g. White & Bolton, 2005).

4.3. Comparison of load test results and estimation results on full-scale RCP piles

The calculation was conducted with dz in equation (6) being 0.1m. The values of SPT N were interpolated linearly with depth, but were not averaged over a depth range. The unit weight of soil (γ) was assumed to vary from 14 to 20 depending on the soil type. The internal friction angle of soil (ϕ) was estimated by equation (27) (RTRI, 2013) where σ_v*'* is the effective overburden pressure, and the friction angle at the soil-pile interface (δ_{sp}) was assumed to be two-thirds of ϕ. β was obtained either by equation (24) or (26), with K varied from 0.3 to 0.6.Values of N at or deeper than 18.3m in Site T were assumed to be 50. Regarding A-2016, to account for the change of installation techniques (from Rotary Cutting Press-in to Standard Press-in) at z = 2.0m, the method in Fig. 6 was adopted for 0m $\le z <$ 2.0m while that in Fig. 5 was adopted for $z \ge$ 2.0m.

$$\phi = 1.85\left(\frac{N}{0.01\sigma_v' + 0.7}\right)^{0.6} + 28 \tag{27}$$

Fig. 14 shows a comparison of the measured and estimated values of h during Rotary Cutting Press-in. Measured h values were comparable to z in every test, implying that the pile was installed in an almost fully unplugged manner. It can be confirmed that the estimated h agrees with the measured trend in each test. The transition of the plugging condition at 5m<z<10m in F-2009 is well reproduced. Looking at the results more closely, a slight underestimation can be found in T-2009 and N-2017. Considering that these underestimating trends appear where soft fine soils exist, one reason might be the effect of pore water pressure. Excess pore water pressure generated around the pile base during installation in soft (contractile) fine soils might have increased the base stress (q_{bi}) and reduced the frictional stress (τ_i), which allows easier invasion of the soil from beneath the pile base to inside the pile. Regarding the influence of β values, equation (24) and equation (26) with K=0.3 provide similar results. Increasing the value of K in equation (26) has little influence on the estimated h, except for z>7m in A-2016. It is suggested that the reduction of τ_i due to rotation, as expressed by equation

(19), is much more influential than the variation of K from 0.3 to 0.6.

Fig. 15 shows a comparison of *FFR* values estimated by UWA-05 (equation (7)) and the proposed method. *FFR* estimated by the proposed method varies with depth, while that estimated by UWA-05 does not. Focusing on the depths of pile base where load tests were conducted (indicated by dotted lines in Fig. 15), *FFR* estimated by the proposed method are similar to those estimated by UWA-05. The influence of β values is small at these depths, while it becomes greater with depth in some depth ranges (10m<z<15m and z>18m in T-2007, 10m<z<20m in N-2017 and 4m<z<9m in A-2016).

Fig. 16 shows a comparison of measured and estimated values of $Q_{b,0.1Do}$. The depth ranges where β values are influential to $Q_{b,0.1Do}$ correspond to those where they are influential to *FFR*. At the depths of pile base where load tests were conducted, the influence of β values is relatively small, and the estimated values are in good agreement with the measured values except for the 10-20% underestimation in F-2009. This underestimation is due to the overestimation of *IFR* (and *FFR*) in 12m<z<15m, which can be confirmed by comparing the inclination of the estimated h-z curves in Fig. 14 with that of the trends of the measured plots in 12m<z<15m. One reason for this would be the dilatancy of sands. The proposed method assumes that the vertical stress acting on the upper plane of the infinitesimally thin disk of soil at the bottom of the soil column (p) does not exceed the maximum value of the base stress experienced previously (q_{BI}). If the soil above the disk shows positive dilatancy, however, p would exceed q_{BI}, leading to smaller *IFR* and greater $Q_{b,0.1Do}$.

Comparison of $Q_{b,0.1Do}$ measured in the load tests and that estimated by IPA (2014) and the proposed method is summarized in Fig. 17. Up to 50% underestimation is found in IPA (2014), while better agreement can be confirmed in the proposed method. Adopting equation (24) or equation (26) with K=0.3 provides generally conservative estimation. Taking K as 0.6 provides the best correlation with the measured values but leads to up to 15% overestimation in some cases.

5. Effects of analysis parameters

5.1. Averaging of SPT N

In design, it is usually the case that the values of q_c or N averaged over a certain depth around the pile base are adopted to estimate $q_{b,0.1Do}$. In this sub-section, the influence of three averaging methods will be investigated. The first uses the linearly interpolated value at the depth of the pile base without averaging, as adopted in Section 4 (‘Not averaged’). The second applies a simple arithmetic averaging to the values from the pile base to 3D_o below the pile base (‘Averaged (0～3D_o)’) as recommended in JRA (2017). The third averages from 4D_o above to 1D_o below the pile base (‘Averaged (-4～1D_o)’) as recommended in AIJ (2001).

Fig. 18 shows a comparison of $Q_{b,0.1Do}$ measured in the field tests with those estimated by the proposed method with β values being obtained by equation (26) with K=0.5. It can be confirmed that the influence of the averaging methods is obvious only in the depth ranges where SPT N rapidly varies with depth (especially near the depth of the upper surface of the bearing stratum), hastening or delaying the timing of sensing the bearing stratum. As a result, ‘Averaged in 0～3 D_o’ leads to overestimation and ‘Averaged in -4～1 D_o’ leads to underestimation of $Q_{b,0.1Do}$.

5.2. Other installation factors

Water injection in Rotary Cutting Press-in is believed to be effective in cooling the cutting teeth and preventing damage to them due to high temperature, as well as in smoothening the penetration by building up excess pore water pressure around the pile base and reducing the effective stress, and by lubricating the pile-soil interface and reducing the pile-soil friction inside and outside of the pile. The excess pore pressure effect will influence q_{bi} and τ_i as discussed in Sections 4.1 and 4.3, but this effect was not incorporated into the proposed method.

As discussed in Section 4.3, the effect of dilatancy of sands was also ignored. The proposed method assumes that the vertical stress acting on the upper plane of the infinitesimally thin disk of soil at the bottom of the soil column (p) does not exceed the maximum value of the base stress experienced previously (q_{BI}). If the soil above the disk dilates, p would exceed q_{BI}, leading to smaller *IFR* and greater $Q_{b,0.1Do}$.

The effect of cutting teeth on the pile base was not directly considered in the proposed method. However, it could be interpreted that this effect is implicitly considered by an adoption of small β values based on equation (24) or equation (26) with K=0.3-0.6.

In the static load tests, strain gauge readings were zeroed just before the load tests (after the end of installation). This leads to an uncertainty of the residual stress in the pile and an undermeasurement of $Q_{b,0.1Do}$. On the other hand, the strain gauges for obtaining $Q_{b,0.1Do}$ in the load tests were positioned at some distance above the pile base. This will make the measured values of $Q_{b,0.1Do}$ greater than the base capacity at the very base of the pile. Effects of these two factors were also ignored in this paper.

6. Conclusions

A method to estimate the plugging condition (*IFR* and *FFR*) and the base capacity of RCP piles from CPT or SPT results was proposed, based on the framework of UWA-05. Estimation results were compared with the field test results, and the followings were revealed.

(1) *IFR* during installation is well reproduced by the proposed method, if the ratio of frictional stress to vertical stress inside the pile (β) is estimated appropriately.

(2) The base capacity estimated from SPT results by the proposed method with appropriate β values shows good agreement with the values measured in the load tests than those estimated by IPA (2014).

(3) Assumption of an active failure to obtain β, as proposed by Randolph et al. (1991), gives slightly conservative estimation of base capacity. Taking K as 0.6 in $\beta=K\tan\delta_{sp}$, with K being the coefficient of earth pressure and δ_{sp} being the friction angle at the soil-pile interface, provides the best correlation with the measured values but leads to up to 15% overestimation in some cases.

(4) Averaging SPT N values over a certain depth range, as recommended in many design codes, is not effective in improving the validity of the proposed method.

(5) Water injection during installation, dilatancy of sands in the pile, and cutting teeth on the pile base would have some influence on the estimation results, but were ignored in the proposed method. The effect of residual stress was also ignored in the load tests. Further work is necessary to clarify the extent of the influence of these factors to directly incorporate them into the proposed method, while collecting results from additional field tests to verify it.

Acknowledgements

The authors are grateful to Dr. Yoshiaki Kikuchi and Mr. Takashi Kurashina for advices and cooperation in the model

test quoted in Section 4.1.

References

Architectural Institute of Japan (AIJ). 2001. Recommendations for Design of Building Foundations, 485p. (in Japanese)

Bearing Capacity of Piles (BCP) Committee. 1971. Field tests on piles in sand. Soils and Foundations, Vol. 11, No. 2, pp. 29-50.

Bond, T. 2011. Rotary jacking of tubular piles. M.Eng. Project Report, Cambridge University Department of Engineering, 50p.

Chow, F. C., Jardine, R. J., Brucy, F. and Nauroy, J. F. 1998. Effects of time on capacity of pipe piles in dense marine sand. Journal of Geotechnical and Geoenvironmental Engineering, Vol. 124, No. 3, pp. 254-264.

Deeks, A. D. and White, D. J. 2007. Centrifuge modelling of the base response of closed-ended jacked piles. Advances in Deep Foundations, pp. 241-251.

Dingle, H. 2006. The testing and analysis of jacked foundation piles. M.Eng. Project Report, Cambridge University Department of Engineering, 50p.

Hirata, H., Suzuki, T., Matsui, N. and Yasuoka, H. 2009. Bearing capacity performance of rotary press-in method (Gyropress Method): part 1 (vertical capacity). Proceedings of the 65th JSCE (Japanese Society of Civil Engineers) Annual Meeting, pp. 41-42. (in Japanese)

International Press-in Association (IPA). 2014. Design and Construction Manual for Earth Retaining Walls with Tubular Piles Installed by Gyropress (Rotary Cutting Press-in) Method, 143p. (in Japanese)

International Press-in Association (IPA). 2016. Press-in retaining structures: a handbook, First edition 2016, pp. 4.23-4.24.

Ishihara, Y., Haigh, S. and Bolton, M. D. 2015. Estimating base resistance and N value in rotary press-in. Soils and Foundations, Vol. 55, No. 4, pp. 788-797.

Ishihara, Y., Ogawa, N., Okada, K., Inomata, K., Yamane, T. and Kitamura, A. 2016. Model test and full-scale field test on vertical and horizontal resistance of hatted tubular pile. Proceedings of the Third International Conference Geotec Hanoi 2016 - Geotechnics for Sustainable Infrastructure development, pp. 131-139.

The Japanese Geotechnical Society (JGS). 2002. Method for static axial compressive load test of single piles. Standards of Japanese Geotechnical Society for Vertical Load Tests of Piles, pp. 49-53.

Japan Road Association (JRA). 2002. Specifications for Highway Bridges: Part 1 Common & Part 4 Substructures, 567p. (in Japanese)

Japan Road Association (JRA). 2012. Specifications for Highway Bridges: Part 4 Substructures, 586p.

Japan Road Association (JRA). 2017. Specifications for Highway Bridges: Part 4 Substructures, 569p. (in Japanese)

Kerisel, J. 1961. Deep foundation in sands: variation of ultimate bearing capacity with soil density, depth, diameter and speed. Proceedings of the 5th International Conference on Soil Mechanics and Foundation Engineering, Vol. 2, pp. 73-83. (in French)

Kurashina, T. 2016. Model pile penetration test on the mechanism of mobilization of base capacity of an open-ended pile. Master's thesis, Tokyo University of Science, 106p. (in Japanese)

Lehane, B. M. and Gavin, K. G., 2001. Base resistance of jacked pipe piles in sand. ASCE Journal of Geotechnical and Geoenvironmental Engineering, Vol. 127, No. 6, pp.473-480.

Liyanapathirana, D. S., Deeks, A. D. and Randolph, M. F. 2001. Numerical modelling of the driving response of thin-walled open-ended piles. International Journal for Numerical and Analytical Methods on Geomechanics, Vol. 25, No. 9, pp. 933-

953.

Meyerhoff, G. G. 1956. Penetration tests and bearing capacity of cohesionless soils. Journal of the Soil Mechanics and Foundations Division, Vol. 82, Issue 1, pp. 1-19.

Meyerhoff, G. G. and Valsangkar, A. J. 1977. Bearing capacity of piles in layered soils. Proceedings of the 8th International Conference on Soil Mechanics and Foundation Engineering, Vol. 1, pp. 645-650.

Railway Technical Research Institute (RTRI). 2013. Design Standards for Railway Structures and Commentary (Earth Structures). (in Japanese)

Randolph, M. F., Leong, E. C. and Houlsby, G. T. 1991. One-dimensional analysis of soil plugs in pipe piles. Geotechnique, Vol. 41, No. 4, pp. 587-598.

Skov, R. and Denver, H. 1988. Time-dependence of bearing capacity of piles. Proceedings of the Third International Conference on Application of Stress-Wave Theory to Piles, pp. 1-10.

White, D. J. and Bolton, M. D. 2005. Comparing CPT and pile base resistance in sand. Proceedings of the Institution of Civil Engineers, Geotechnical Engineering 158, pp. 3-14.

White, D. J. and Deeks, A. D. 2007. Recent research into the behaviour of jacked foundation piles. Advances in Deep Foundations: International Workshop on Recent Advances of Deep Foundations (IWDPF07), Kikuchi, Yoshiaki, Otani, Jun, Kimura, Makoto and Morikawa, Yoshiyuki (eds.), Japan. CRC Press. pp. 3-26.

White, D. J., Deeks, A. D. and Ishihara, Y. 2010. Novel piling: axial and rotary jacking. Proceedings of the 11th International Conference on Geotechnical Challenges in Urban Regeneration, London, UK, CD, 24p.

Xu, X., Schneider, J. A. and Lehane, B. M. 2008. Cone penetration test (CPT) methods for end-bearing assessment of open-and closed-ended driven piles in siliceous sand. Canadian Geotechnical Journal, Vol. 45, No. 8, pp. 1130-1141.

Yetginer, A. G., White, D. J., Bolton, M. D. 2006. Field measurements of the stiffness of jacked piles and pile groups. Geotechnique 56, No. 5, pp. 349-354.

Short title is appeared here.

List of notations

$A_{b,closed}$	Cross-sectional area of the closed-ended pile
D_i	Inner diameter of the pile
D_o	Outer diameter of the pile
D_r	Relative density of the soil
F	Jacking force applied to the pile
FFR	Final Filling Ratio (the value of IFR at the end of installation)
F_t	Jacking force recorded in the axial loading at the end of installation
F_{UL}	Upper limit of F
f_w	Flowrate of water injected near the pile base
h	Length of the soil column inside the pile
IFR	Incremental Filling Ratio
K	Coefficient of earth pressure
l_d	Downward displacement of the pile
l_t	Pile displacement recorded in the axial loading at the end of installation
l_u	Upward displacement of the pile
N	SPT N value
N_{a1}	SPT N value averaged by a method recommended by JRA (2012)
N_{a2}	SPT N value averaged by a method recommended by JRA (2017)
n_T	Number of cutting teeth on the pile base
p	Vertical stress on the upper plane of the thin disk of soil at the bottom of the soil column
q_{bi}	Stress on the bottom of the soil column inside the pile
q_{bi}'	Effective stress on the bottom of the soil column inside the pile
q_{BI}	Maximum value of q_{bi} observed previously (at shallower depths than the present depth of the pile base)
$q_{b,pl}$	Unit base capacity defined by a plunging load
$q_{b,0.1Do}$	Unit base capacity defined at the pile base displacement of $0.1D_o$
Q	Load applied on the pile head
$Q_{b,0.1Do}$	Base capacity at a pile base displacement of $0.1D_o$
Q_{si}	Total frictional force on the inner surface of the pile
q_c	CPT cone resistance
$q_{c,ave}$	CPT cone resistance averaged by the Dutch method
T	Torque applied to the pile
t_{LT}	Time from the end of installation to the start of load test
T_{UL}	Upper limit of T
v_d	Vertical downward velocity of the pile
v_r	Rotational velocity of the pile surface
z	Depth of the pile base

z_{bs}	Embedment depth into the bearing stratum
β	Coefficient linking q_{bi}' and τ_i
γ	Unit weight of soil
γ_w	Unit weight of water
δ_{sp}	Friction angle at the soil-pile interface
λ	Coefficient linking q_{bi} and q_c
σ_v'	Effective overburden pressure
τ_i	Frictional stress mobilized at the soil-pile interface inside the pile
ϕ	Internal friction angle of soil

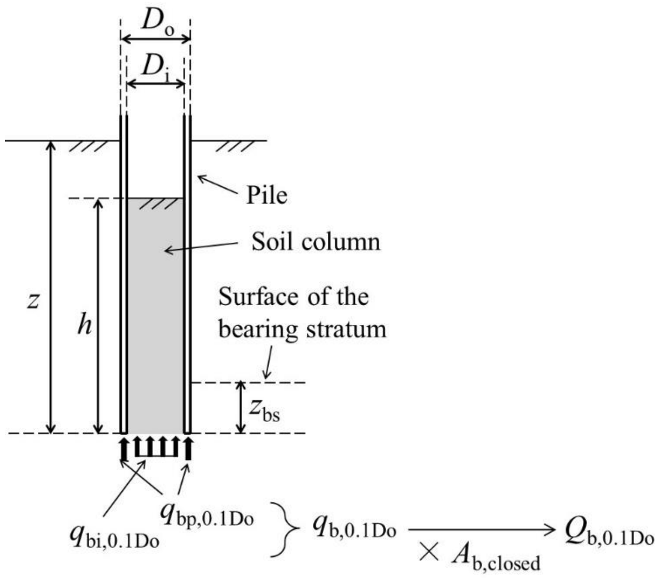

Fig. 1　Symbols related with base capacity

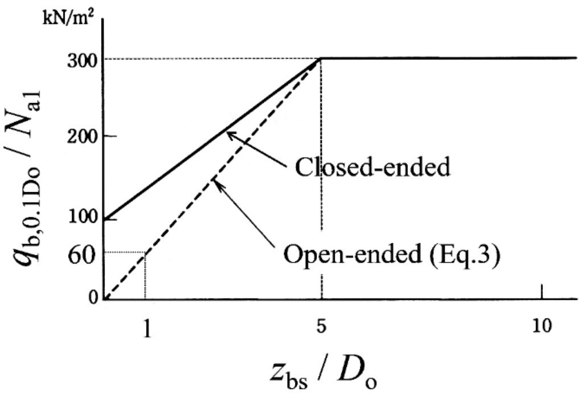

Fig. 2　Reduction of $q_{b,0.1Do}$ with z_{bs} (after JRA (2012))

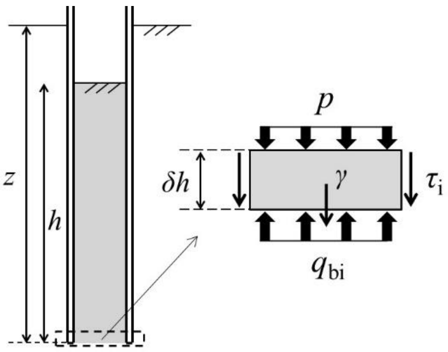

Fig. 3　Infinitesimally thin disk of soil at the bottom of the soil column

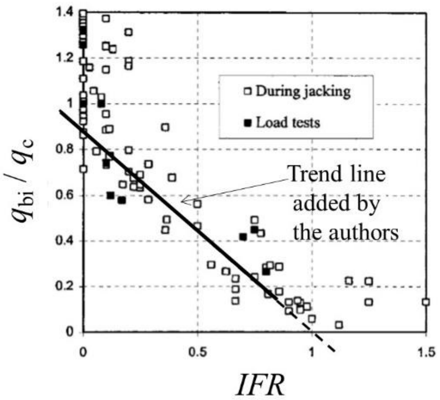

Fig. 4 Correlation between q_{bi}/q_c and *IFR* (after Lehane & Gavin, 2001)

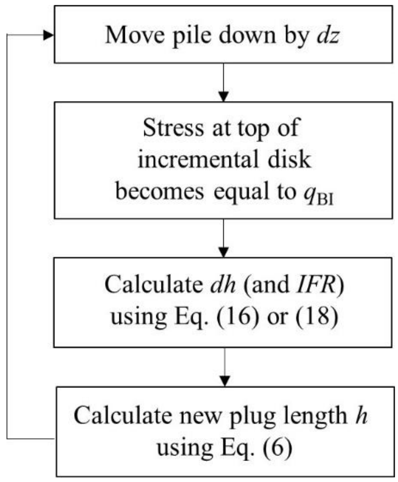

Fig. 5 Procedure for estimating *FFR* of jacked piles from SPT *N*

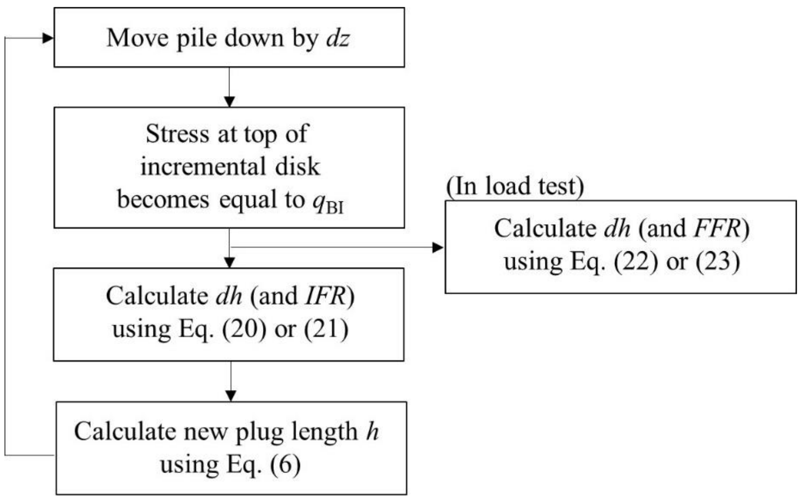

Fig. 6 Procedure for estimating *FFR* of RCP piles from SPT *N*

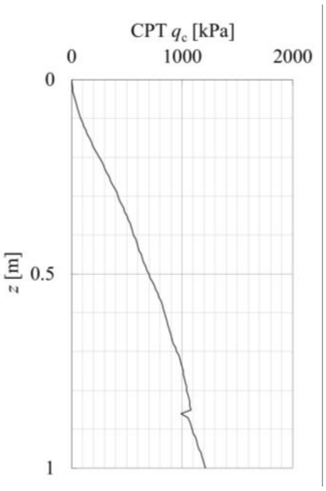

Fig. 7　CPT profile of the model ground

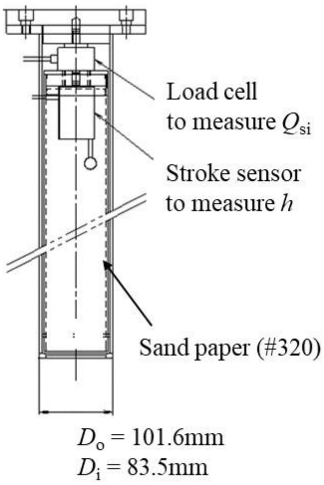

Fig. 8　Test pile used in the model test

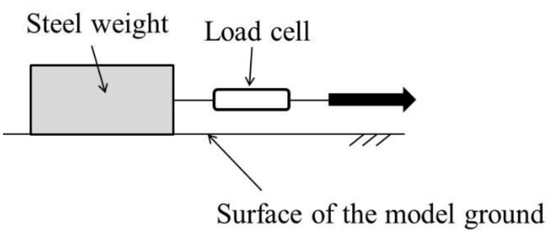

Fig. 9　Simple investigation to estimate δ_{sp}

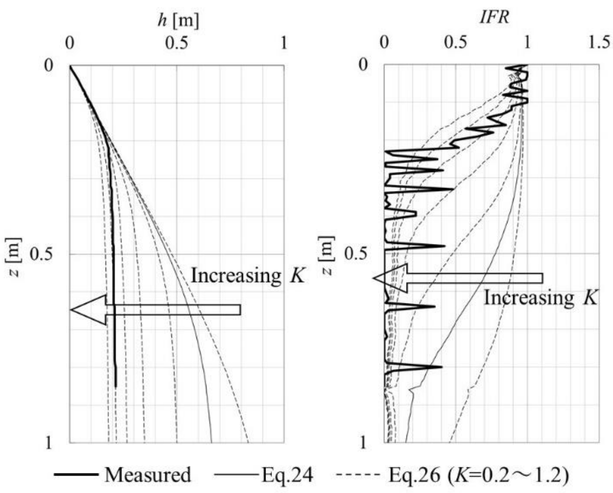

Fig. 10　Comparison of measured and estimated h and IFR

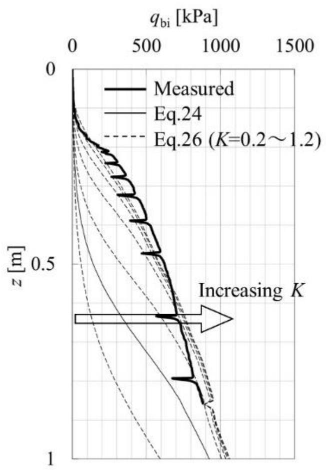

Fig. 11　Comparison of measured and estimated q_{bi}

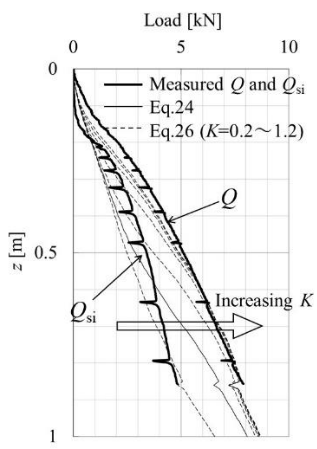

Fig. 12　Comparison of measured Q_{si}, Q and estimated $Q_{b,0.1Do}$

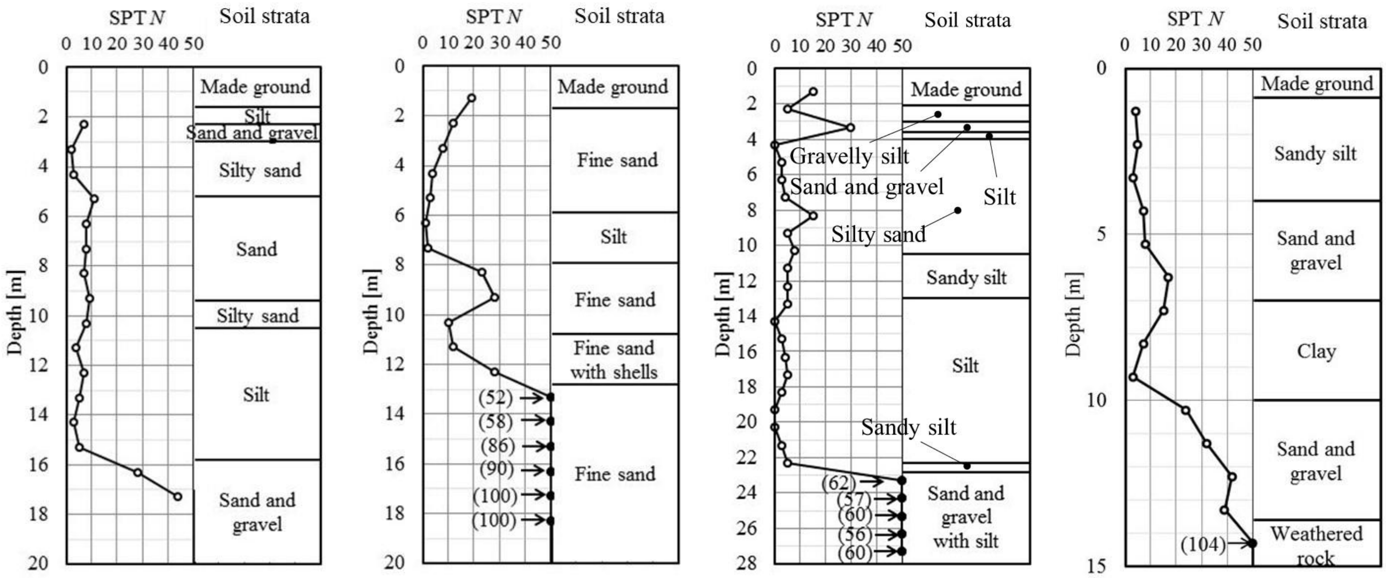

(a) T-2007 (b) F-2008 (c) N-2017 (d) A-2016

Fig. 13 Site profiles

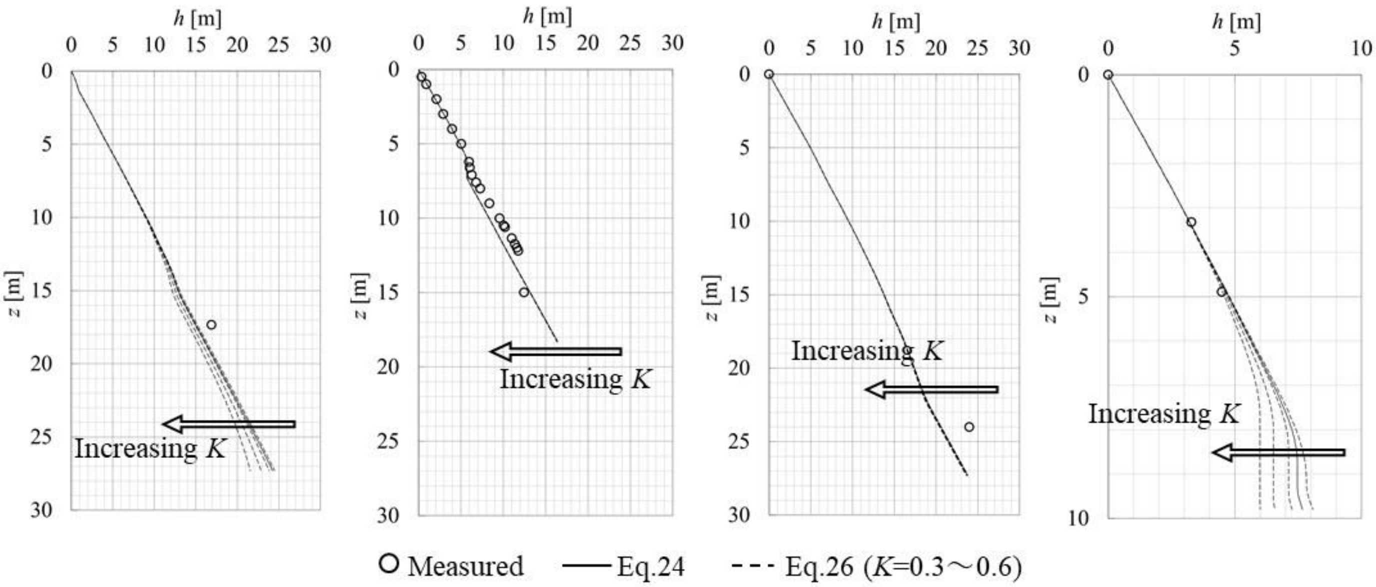

(a) T-2007 (b) F-2008 (c) N-2017 (d) A-2016

Fig. 14 Comparison of measured and estimated h

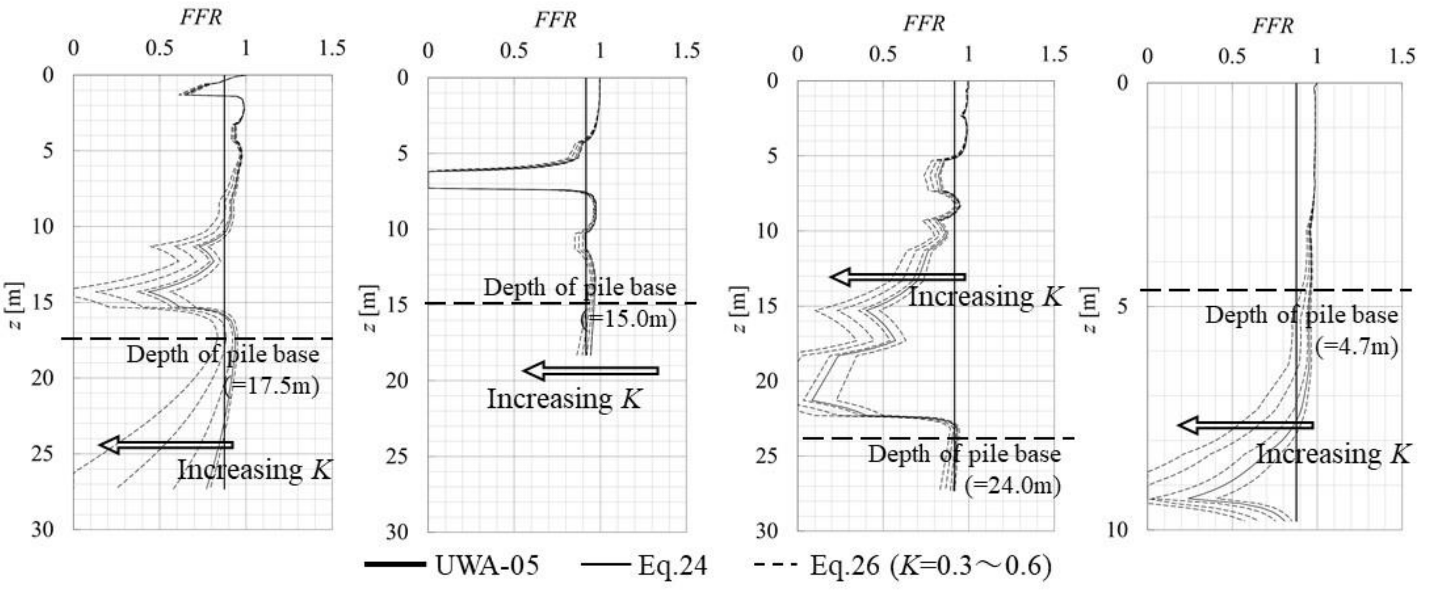

(a) T-2007 (b) F-2008 (c) N-2017 (d) A-2016

Fig. 15 Comparison of UWA-05 and the proposed method in estimating *FFR*

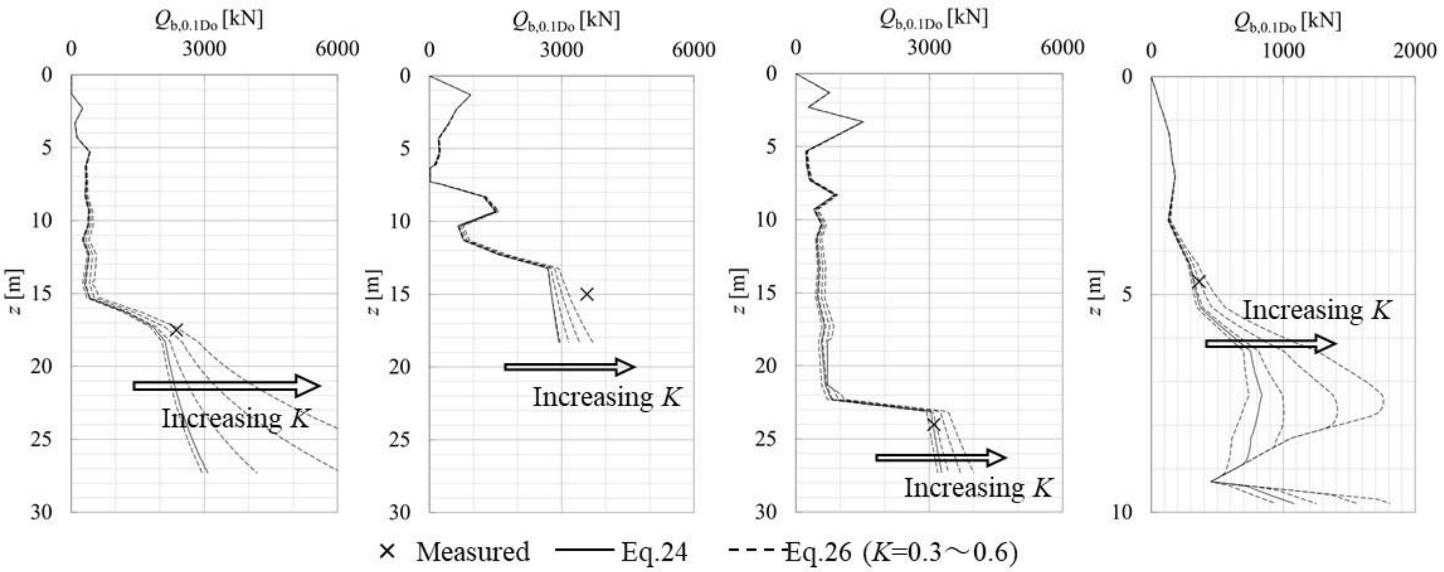

(a) T-2007 (b) F-2008 (c) N-2017 (d) A-2016

Fig. 16 Comparison of measured and estimated $Q_{b,0.1Do}$ of RCP piles

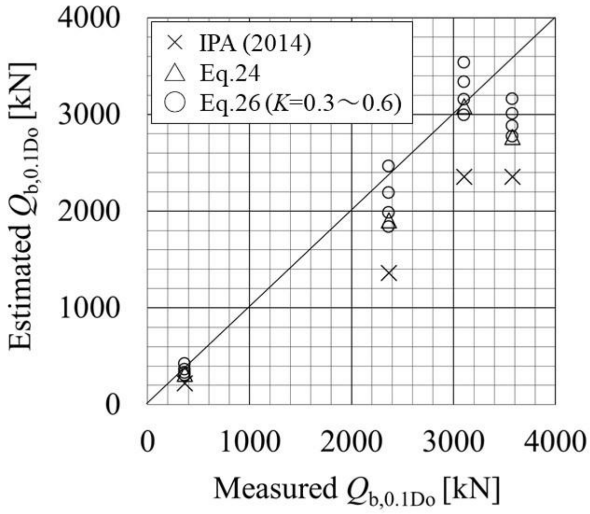

Fig. 17 Comparison of IPA (2014) and the proposed method in estimating $Q_{b,0.1Do}$

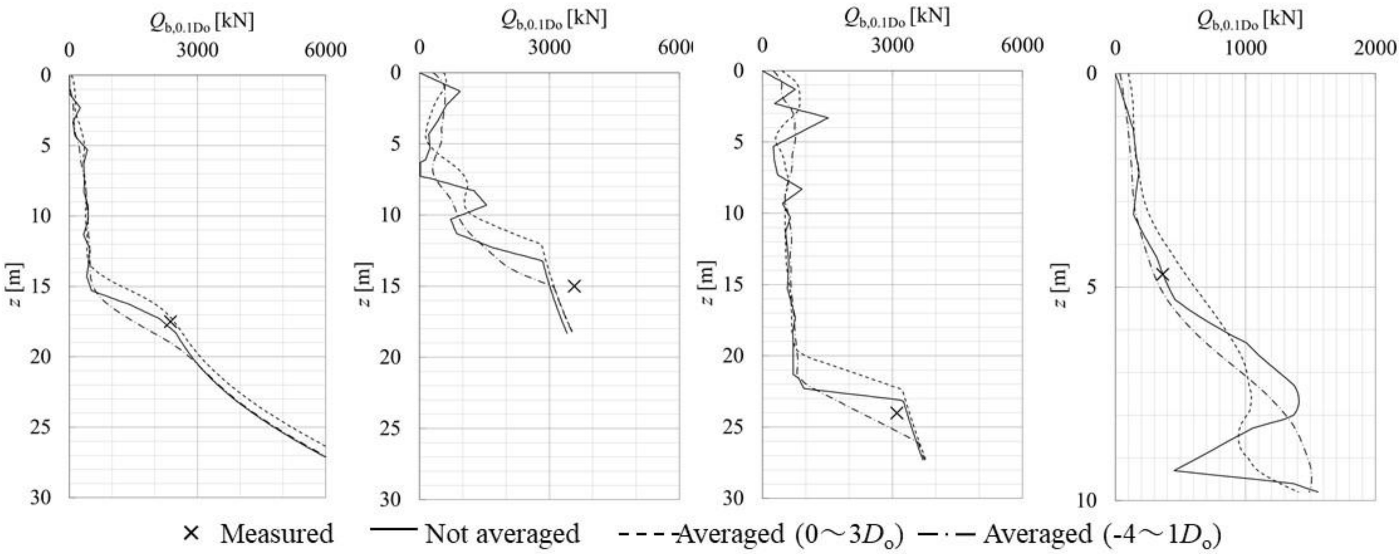

(a) T-2007 (b) F-2008 (c) N-2017 (d) A-2016

Fig. 18 Measured and estimated Q_{bf} with different averaging techniques

Table 1 Pile specifications and installation conditions in static load tests

	D_o	D_i	F_{UL}	T_{UL}	l_d	L_u	v_d	v_u	v_r	n_T	f_w	F_t	l_t
	[mm]		[kN]	[kNm]	[mm]		[mm/s]				[l/min.]	[kN]	[mm]
T-2007	800	768	400-1000	400	300	100	25	66	126	4	10-30 (minimized in the last $1D_o$)	1530	4.0
F-2008	1000	976	500-1000	-	300	100	14	66	157	5	20-30 (minimized in the last $1D_o$)	1709	4.8
N-2017	1000	976	200-1000	250-400	Arbitrary		8	33	367-576	6	15 (minimized in the last $0.9D_o$)	950	3
A-2016	800	776	300	300	Arbitrary		Arbitrary (no rotation below 2m)			4	0	-	-

Table 2 Conditions and results of static load tests

	Method of load test	Loading method	Depth of pile base [m]	Elapsed time, t_{LT} [days]	Base capacity [kN]
T-2007	Static	Multi cycle, step loading	17.5	15	2368
F-2008	Static	Multi cycle, step loading	15.0	14	3576
N-2017	Static	Multi cycle, step loading	24.0	56	3102
A-2016	Static	Multi cycle, step loading	4.7	1.08	363